Atmos. Chem. Phys. Discuss., 10, 21357–21389, 2010
www.atmos-chem-phys-discuss.net/10/21357/2010/
doi:10.5194/acpd-10-21357-2010

Atmospheric Chemistry and Physics Discussions

Large scale modeling of the transport, the chemical transformation and the mass budget of the sulfur emitted during the eruption of April 2007 by the Piton de la Fournaise

P. Tulet[1,2] **and N. Villeneuve**[3,4]

[1]LACy, CNRS, Université de la Réunion, Météo-France, UMR 8105, 15 avenue René Cassin, 97715 Saint-Denis, France
[2]CNRM/GAME, CNRS, Météo-France, URA 1357, 42, Avenue Gaspard Coriolis, 31057 Toulouse, France
[3]CREGUR, Université de La Réunion, 15 avenue René Cassin, 97715 Saint-Denis, France
[4]US140 ESPACE, Centre IRD de La Réunion, BP172, 97492 Saint-Denis, France

Received: 15 July 2010 – Accepted: 31 August 2010 – Published: 8 September 2010

Correspondence to: P. Tulet (pierre.tulet@meteo.fr)

Published by Copernicus Publications on behalf of the European Geosciences Union.

Abstract

During April 2007, the Piton de la Fournaise volcano, La Réunion island, entered in its bigger eruption registered at least one century. Due to the absence of rapid captor in the vicinity of the volcano, the estimation of the degassing during the paroxysmal phase of the event has not been estimated. A modeling study that uses the mesoscale chemical model MesoNH-C, the spatial observation from the OMI sensor and the CALIOP spacelidar, have simulated the global mass of SO_2 observed and the general shape of the SO_2 plume spreading over the Indian ocean. Moreover, an analysis of the budget of the SO_2 plume have permitted to estimate the total SO_2 release to 159 Kt, the transformation in H_2SO_4 at 46.9 Kt and the surface dry deposition to 22 Kt and 17.9 Kt of SO_2 and H_2SO_4 respectively. Then, this top down approach has retrieved an estimation of the temporal evolution of the SO_2 emission during the most active period of the eruption, where the peak of degassing is estimated to 2000 $kg\,s^{-1}$ in the morning of the 6 April. This temporal evolution of SO_2 emission, given here, can also be used for more local studies.

1 Introduction

Volcanoes represent one of the most important natural sources of pollutants in the atmosphere, both during and between eruptions (Mather et al., 2005). Large explosive eruption such as El Chichòn in 1982 (Pollack et al., 1983; Hoffman, 1987) or Mount Pinatubo in 1991 (McCormick and Trepte, 1995; Robock, 2002) have highlight their impacts on the earth radiative balance through the injection of large quantities of aerosol in the troposphere and the lower stratosphere (Delmelle et al., 2002; Oppenheimer et al., 2003; Arellano et al., 2008). In addition, volcanic emission can also cause important perturbation in the air traffic as happens recently during the 2010 Eyjafjöll's eruption in Island (Seifert et al., 2010). For these reasons, the understanding and the forecasting of the volcanic plumes still a major challenge for atmospheric sciences and risks.

ACPD
10, 21357–21389, 2010

In this field, SO_2 is the most measured volcanic gas (Thomas et al., 2009). Resulting to the oxidation of the sulfur present in the magma, the degassing of SO_2 is a good indicator for eruptive activity and also to understand magma storage and the process of transfer into the atmosphere (Edmonds et al., 2003; Sutton et al., 2001). In the atmosphere, oxidation of SO_2 into sulfate form aerosols by homogeneous nucleation (Kulmala et al., 1998) or deposition on pre-existing aerosols (Seinfeld and Pandis, 2006; Martin et al., 2008; Stevenson et al., 2003). By aqueous processes, SO_2 can also form acid rain (Hoffman et al., 1985; Stevenson et al., 2003). Globally (Penner et al., 2001) have estimated that the budget of volcanic SO_2 burden in atmosphere ranging from 6 to 20 Tg of sulfur per year ($TgS\,yr^{-1}$). This amount of release is non negligible in comparison to anthropogenic flux range estimated at 70 to 100 $TgS\,yr^{-1}$ (Penner et al., 2001) which correspond to 70% of the total sulfur emissions.

Since long time satellite-based measurements of volcanic SO_2 emissions were, however, limited to major eruptions linked with large production of SO_2 and big plume (Carn et al., 2008). Until recently, most of measurements of volcanic SO_2 flux between two eruptive crises or for low emissions during eruptions of effusive volcanoes and volcanoes with a Volcanic Explosively Index greater than 4, were based on ground or airborne instrumentation (Carn et al., 2007). Even if most space-based SO_2 measurements were very useful for volcanic hazard mitigation (including aviation consequences) and volcanic clouds tracking long distance from source (Krueger et al., 1995; Afe et al., 2004; Khokhar et al., 2005), a significant advance was introduced with new sensors (Carn et al., 2008).

In this context, the release of SO_2 in the atmosphere generated by the eruption of the Piton de la Fournaise in April 2007 at La Réunion need to be estimated for two reasons. First, the Piton de la Fournaise is one of the world's most active volcanoes (Lenat and Bachelery, 1987) with an average of one eruption every eight months during the last fifty years (Peltier et al., 2009). Second, the April 2007 eruption is the largest eruption of the Piton de la Fournaise for at least one century (Deroussi et al., 2009). The total amount of magma has been estimated at $180 \times 10^6\,m^3$ ($90 \times 10^6\,m^3$ on Grand Brûlé

ACPD
10, 21357–21389, 2010

area (Staudacher et al., 2009) and 90×10^6 m^3 into the sea (SaintAnge, 2009).

The Piton de la Fournaise is not a volcano known for its ability to produce volcanic plumes of ash and sulfur. In literature, only few examples are references to such activity. Most often associated with historic collapses, this kind of activity is principally characterized by the presence of volcanic ash. Khokhar et al. (2005) is the only reference with an observation of a plume rich in sulfur produced by an eruption of the Piton de la Fournaise. During whole the April 2007 eruption no ground-instrument that quantify continuously SO_2 was installed. As a consequences, the degassing of the Piton de la Fournaise, has not been estimated during the paroxysmal stage. The main objective of this study is to estimate the release of SO_2 using both a large scale satellite observations and a modeling top-down approach. This paper is organized upon five sections. The first section focuses on the eruption phenomenology. An analysed of the SO_2 plumes observed by satellites is reported in the second section. Then, the numerical methods (Sect. 3) and the simulation results (Sect. 4) are presented. The last section is devoted to quantifies the mass budget of the volcanic sulfur and to gives an estimation of the SO_2 emitted during the main eruptive period.

2 Description of the April 2007 Piton de la Fournaise volcano eruption

The 2 April 2007 eruption is the largest eruption of the Piton de la Fournaise volcano, in La R'eunion island for at least one century (Deroussi et al., 2009). The new collapse of summit caldera caused significant morphological change (Michon et al., 2007). Due to this abnormal phenomenology and the large impact on the environment and on civil protection policy, this eruption is very well described on literature. Most important phases are here summary. The 2 April 2007 eruption was preceded by two short eruptive events (only several hours) on 18 February and on 30 March. At 06:00 UTC on 2 April, a new eruption started along a 1 Km fissure, located on the lower south-eastern part of the Enclos (called Grand Brûlé) at only 590 m a.s.l. 7 Km away from the summit and 3 Km from the coast. The beginning of 2 April 2007 eruption was characterized

ACPD
10, 21357–21389, 2010

on field by 50 m high continuous lava fountains feeding voluminous lava flows (Michon et al., 2007). This phenomenology is related to high seismicity recorded from the opening of the eruptive fissure by the whole network Observatoire Volcanologique du Piton de la Fournaise (Staudacher et al., 2009). During few hours on 3 April activity dramatically decreases before re-increases gradually till reach its maximum at mid-day on 6 April. This was contemporaneous with remote sensed observation. Indeed, Coppola et al. (2009) have estimated by radiance analyses on MODIS sensors a significant increase of the rate flow between 3 and 5 April, respectively from 55 to 75 $m^3 s^{-1}$. The first implication of the location of the vent near the coast was the very fast and early entrance of the voluminous lava flow into the sea. This had as effect to produce a large acid water vapour plume (pH lower than 2), rich in chlorine, Sulfur, Pélés hair and rock particles spitted with the thermal shock between lava at about 1480 K and seawater (Staudacher et al., 2009). On 5 April at 20:48 UTC an earthquake of magnitude 3.2 occurred. It was contemporaneous with the beginning of caldera formation (Michon et al., 2007). It is also convenient with the geodesic network measurements. Whole the GPS network recorded first an inward deformation since the beginning of the 5 April afternoon until 20:48 UTC, then a sudden outward displacement of 10–20 cm (Peltier et al., 2009). From 5 April, at 20:48 UTC and until 7 April, at 00:00 UTC , the activity changed (Michon et al., 2007). Analysis of geophysical network signals allows to determine cycles characterized by variations of seismic activity and by deformation (progressive inward displacement ending in a strong outward motion) (Michon et al., 2007, 2009; Staudacher et al., 2009; Peltier et al., 2009). Those authors interpreted cycles as expression of pressure variations in the magma chamber causing sequential formation of the caldera. Output rate flow had been estimated with a maximum during the 6 April by field observation (greater to 200 $m^3 s^{-1}$) (Coppola et al., 2009). We consider that this value is clearly underestimated. Nevertheless, observations clearly shown that the maximum of activity on the eruption field (higher degassing, higher lava fountains and higher output rate flow) was coeval to the higher seismic activity signature. Figure 1 illustrates very well the volcanic phenomenology during the maximum stage. Figure 1a

ACPD
10, 21357–21389, 2010

and b show the evolution between the afternoon of the 5 April (Fig. 1a) when the activity increased and the afternoon of the 6 April (Fig. 1b) at the end of the collapses period. For the Fig. 1d, the photographer was installed near the Piton des Neiges summit at 27 Km far from the Piton de la Fournaise summit and 37 Km far from the sea line (at the Grand Brûlé). The ash plume (gray) close to the Piton de la Fournaise summit is linked to one of the sequential collapses. Note that this ash plume is small in term of extension. The SO_2 plume (orange) was link to the degassing (event and lava flow field). As its explained latter in the text its spreading is control in altitude. Then, the water vapour plume (white) was link to the lava flow entrance into the sea. Note on the Fig. 1c that the field activity dramatically decreases and that the lava reached it maximum lateral and longitudinal extension. From 8 April and till 1 May, even if the activity remains relatively high on the beginning, this stage of eruption phenomenology was more classical. On 10 April between 08:00 and 11:00 UTC a rapid decrease of seismicity of intensity was followed by a break during 8 h. From 19:00 UTC activity reappeared. On 12 April between 11:00 and 14:00 UTC a new collapse coevals with an important output rate flow and a small ash plume dispersion. Then activity remained stable until the end of the eruption.

3 Large scale transport of SO_2

3.1 Integrated profile from OMI

The NASAs EOS/Aura satellite has on-board the sensor OMI that is able to retrieve the SO_2 integrated column. Theretrieval method used in this study, follows the algorithm described by Krotkov et al. (2006); Yang et al. (2009) and has been validate by Krotkov et al. (2008). OMI SO_2 level 2 data products ($OMSO_2$ V003) used in our analyses are available on the NASAs Goddard Earth Sciences Data and Information Services Center web page (http://disc.sci.gsfc.nasa.gov/Aura/data-holdings/OMI/omSO2_v003.shtml).

ACPD
10, 21357–21389, 2010

The evolution of SO_2 column have been superimposed on meteosat satellite picture (visible channel) for the period 4 to 9 April, 2007 (Fig. 2) in order to illustrate the regions where clouds cover can prevents the OMI observations. For 4 and 5 April, SO_2 burden measurements have been determined at the Lower Tropospheric Level plume (TRL) which corresponds to a center mass altitude of 2500 m a.s.l. (OMI Data User's Guide V003, http://disc.sci.gsfc.nasa.gov/Aura/data-holdings/OMI/omSO2_v003.shtml) (Fig. 2a and b). For the rest of the eruptive period, the Middle tropospheric SO_2 column (TRM), corresponding to CMA of 7500 m a.s.l. has been used (Fig. 2c to f). These choices are explained by a greater presence of SO_2 in the mid-troposphere after the6 April (see next section).

The presence of cloudy area inhibits the detection. In these regions, the SO_2 burden observed in Fig. 2) corresponds to the mass located over the top of the clouds. As a consequences, clouds leads an underestimation of measured values of SO_2. Sometimes some pixels values can be negative due to possible problems on measurement. It is also convenient to Georgoulias et al. (2009) observations who assumed that negative SO_2 total column values are link to a low amount of SO_2. These non-physical values have been removed in Fig. 2. This explains the lack of pixels in different locations of the plumes. On 4 April, the SO_2 plume observed by OMI at 11:00 UTC is low, reaching 1 Dobson Unit (1 DU corresponding to 2.68×10^{16} molecules cm^{-2}) and spreading about 2° west from La Réunion. The SO_2 increases on 5 April, at 10:00 UTC, reaching 50 DU at the west of La Réunion. The SO_2 also has been advected at a long distance at the west, close the east coast of Madagascar, where the value of SO_2 is close to 2 DU.

6 April (11:00 UTC) is the day when the Piton de la Fournaise main summit crater (Dolomieu) collapsed, and important quantities of lava have been emitted (Sect. 2). Unfortunately, this day is also marked by the presence of clouds over La Réunion area that prevents a complete detection of the SO_2 by OMI (Fig. 2c). Indeed the maximum value of 12 DU observed in this area is probably largely underestimated and corresponds to the SO_2 located above the clouds. Nevertheless one can note on Fig. 2c that the

ACPD
10, 21357–21389, 2010

plume is intensified and spreaded toward the west, close to east coast of Madagascar, the north and east of La Réunion reaching the Maurice Island (15 DU). Considering that the low troposphere winds (alizes) (Diab et al., 2004) are directed from southeast to northwest, the presence of the plume on eastern and northern area of La Réunion indicates that SO_2 plumes have been transported above to the inversion layer where winds are reversed. In 7 April at 10:00 UTC (Fig. 2d), the plume observed by OMI is intense, advected through the north of La Réunion and then moving eastward. The plume is detected at the longitude 83° that represents a distance over 2800 Km from the Piton de la Fournaise. The integrated column of SO_2 is important, with 50 DU over La Réunion island, 40 DU in the northern branch and about 15–20 DU in the eastern branch until 65° of longitude. A gap in the plume shape is notable on northern area of Maurice island. It is probably due to the presence of clouds. Close to Madagascar a second SO_2 (2 DU) plume corresponds to the western branch of the 6 April plume. The importance of SO_2 plume detected far from La Réunion suggests that the SO_2 release on 6 April have been important.

The 8 and 9 April, the plume SO_2 decreases with a maximum of 7 DU (Fig. 2e) and 12 DU (Fig. 2f) respectively. This second maximum at 12 DU located at latitude −16° and longitude 58° is puzzling given the fact that no such strong values have been observed upstream in the plume on 8 April. Thus, it implies that some plumes of SO_2 have been masked by the presence of clouds. In this latter period, the plume extended over Indian Ocean from longitude 48° on 8 April, to longitude 95° on 9 April (not shown). Above Madagascar, the presence of a cloud system seems to interact with the western part of the plume.

3.2 Plumes altitudes from CALIPSO

An analysis of the location of each aerosol plumes observed by the different passages of CALIPSO between 2 and 11 April have been reported on Fig. 3 in function of their distance from La Réunion and their altitude. On CALIPSO satellite, the Cloud-Aerosol Lidar with Orthogonal Polarization (CALIOP) provides high-resolution vertical profiles

ACPD
10, 21357–21389, 2010

(100 m footprint size) of aerosol and clouds. This sensor allows the discrimination of cloud phase and the identification of the presence of non-spherical aerosols (Winker et al., 2003; Carn et al., 2007). CALIPSO completes 14.55 orbits per day with a separation of 24.7° longitude between each successive orbit at the equator.

Here, it is assumed that the aerosol plumes observed are formed by the sulfur oxidation into sulfuric acid (through homogeneous nucleation or by deposition on pre-existing aerosol, Seinfeld and Pandis, 2006). This assumption based primarily on the fact that there is no other important source of aerosol over the Indian Ocean during this period, except sea salt in the boundary layer.

On 3 and 4 April, CALIPSO track has crossed the Piton de la Fournaise's volcanic plumes in the western vicinity of La Réunion lower than 3000 m a.s.l. This imply that there is no important uplift of the SO_2 over La Réunion and the volcanic plume still located in low troposphere level. From 6 April, due to the very intense volcanic activity the volcanic plumes crossed the inversion layer. As explained in Sect. 5, plumes change their global direction, they spread toward east and reach the mid and upper troposphere. On 6 April, CALIOP sensor detected three aerosol plumes close to La Réunion at 5500 m a.s.l., 6500 m a.s.l. and 7500 m a.s.l. The altitude of these plumes indicates that an important uplift has transported the SO_2 into the mid-troposphere. On 7 April, two aerosol plumes have been also observed in altitude while the LIDAR provides transects at 800 Km (5500 m a.s.l.) and 1800 Km (7300 m a.s.l.) in east from La Réunion. These plumes correspond probably those observed on 6 April. SO_2 and sulfate aerosol lifetime are longer in upper troposphere compare to lower atmosphere (Stevenson et al., 2003; Yang et al., 2009). Then we assume that the plumes observed on April 6 and 7 are also those observed in east on 8, 9, 10 and 11 April respectively at around 800 and 1100 Km (6500 m a.s.l. and 10 200 m a.s.l.), 1200 Km (6300 m a.s.l.), 1000 Km (9900 m a.s.l.) and 1200 Km (3600 m a.s.l.) from La Réunion. It is also convenient with shapes evolutions of SO_2 plumes observed with OMI. Plumes Altitudes in eastern Indian Ocean suggest that the transport of SO_2 continues the days after the collapse of the crater. The cartography performed using OMI and field observations

ACPD
10, 21357–21389, 2010

allow to validate that higher eastern plumes formed during three days (6, 7 and 8 April). In the western part of the Indian Ocean, between La Réunion and Madagascar, apart on 9 and 11 April (4200 m a.s.l. and 4400 m a.s.l.), plumes were never observed over 3100 m a.s.l. Inversion Layer was not cross by these plumes that was formed by smaller volcanic activity.

4 Simulation and evaluation

4.1 The MesoNH model

The mesoscale-scale, non hydrostatic atmospheric model MesoNH is used in this study. This model has been jointly developed by CNRM (Meteo France) and the Laboratoire d'Aérologie (CNRS) (Lafore et al., 1998). MesoNH can be used to simulate small scale (LES type) to synoptic scale phenomena (horizontal resolution ranging from a few meters to several tens of kilometers), and it can be run in a two-way nested mode involving up to 8 nesting stages. Different sets of parameterizations have been introduced for convection (Bechtold et al., 2001), cloud micro-physics (Cohard and Pinty, 2000), turbulence (Bougeault and Lacarrere, 1989), biosphere-atmosphere thermodynamic exchanges (ISBA) (Noilhan and Mahfouf, 1996), urban-atmosphere interactions(Masson, 2000), lightning processes (Barthe et al., 2005), gaseous chemistry (Suhre et al., 1998; Tulet et al., 2003) and aerosols (Tulet et al., 2005; Grini et al., 2006).

For this study, the ReLACS chemical scheme (Crassier et al., 2000) have been used to represent the sulfur dioxides oxidation and the formation of sulfuric acid.

4.2 Simulation configuration

The simulation started at 00:00 UTC on 4 April 2007, and ended at 00:00 UTC on 11 April 2007. The simulation domain cover a large part of the Indian Ocean between

ACPD
10, 21357–21389, 2010

latitudes 28.6° S and 10.9° S and longitudes 40.78° E and 71.22° E. The horizontal resolution of the model is 20 Km that is complementary to the OMI footprint size (13 Km by 24 Km). The vertical resolution was composed of 60 vertical levels stretched up to an altitude of 24 000 m a.s.l., whereas 30 levels were located in the lower atmosphere between the surface and 1500 m a.s.l. The initial and lateral boundary conditions were taken from ECMWF analysis for the meteorology and from MOCAGE (Peuch et al., 1999) for gas chemistry.

4.3 Estimation of the day by day SO_2 release

The estimation of the gas emission in the atmosphere during this eruption is a hard objective due to the absence of any local rapid observing system of the gas in the vicinity of the volcano. To counterbalance this problem and to put the SO_2 emitted by the eruption in the model, a top-down approach has been adopted. For each days, except the April 6, the SO_2 mass burden characteristicof La Réunion area have been extracted from OMI. Due to the presence of clouds, and the model resolution, the main difficulty was to estimate a characteristic mean value of SO_2 able to be introduce in the model grid. Then, the SO_2 mass burden estimated is converted in homogeneous concentration of SO_2 upon a column of atmosphere located above the eruption (Table 1).

The top altitude of this column have been estimated by two manner: (i) using the aerosol plume observed by CALIPSO (Sect. 3.2), and (ii) to correctly reproduce the form of the SO_2 plume inthesimulation using the fact that the atmosphere is strongly vertically sheared in these regions (Baray et al., 1998; Clain et al., 2009) (Sect. 5).

On 6 April, the lava flux (and the release of the SO_2), is too variable during the day to use the daily value from the satellite. More-over, as explained before, the presence of clouds prevents a correct estimation of the SO_2 by OMI over La Réunion region. For these reasons, the SO_2 concentration introduced for 6 April, are estimated in order to fit, as close as possible the plume observed in 7 April (see Sect. 6). The temporal evolution of the SO_2 vertical concentration has also taking into account the daily tendency of seismicity (Michon et al., 2007).

ACPD
10, 21357–21389, 2010

Moreover, during the major eruptive period, the SO_2 plume has been uplifted by convection and/or forced by the orography of La Réunion. This due to the sensible heat flux (lava surface temperature up to 1000 °C) and the important latent heat flux generated by the water evaporation when the lava has entered in the ocean. In addition, the presence of steep relief (summit up to 3000 m) can modified the alizes flux around La Réunion (Lesouef et al., 2008), and can amplified the convection. These two processes are not reproduced by the model due to the horizontal resolution used (20 Km). The orography is smoothed, and the summit of La Réunion is lowered to 500 m. For these reasons, the choice was to considered the bottom of the SO_2 column above the surface. Several numerical tests has permitted us to adjust the altitudes boundaries of the SO_2 column introduced in the model. All the data introduced in the model have been reported in Table 1. At each time step of the model, a linear temporal interpolation is made between all the data of Table 1.

5 Evolution of the SO_2 plume over the Indian Ocean

5.1 SO_2 mass burden

Figure 4 represent the evolution of the SO_2 mass burden simulated by MesoNH. This figure has to be compared with OMI observations of Fig. 2. As for the satellite observations the first period 4–5 April, show that the plume is oriented in the west. On 5 April, SO_2 mass burden reach 30 DU over La Réunion that is in the same order of magnitude with the OMI observation.

The 6 April, the model is able to reproduce the branches west and east of the SO_2 plume, but the northern observed branches observed by OMI north of Maurice island is not wide enough in the simulation. The plume extending from La Réunion to Maurice island present strong values of SO_2 up to 50 DU. On 7 April, the general shape of the SO_2 distribution is retrieved. As for OMI observations, the western plume has reached Madagascar (Fig. 2d). The main plume of La Réunion (30 DU) is oriented in the north,

ACPD
10, 21357–21389, 2010

and turn on the east of the domain. A second maximum at 30 DU is simulated north of Maurice Island, that corresponds to the maximum emission of SO_2 by the volcano. As for the observations, the SO_2 plume simulated reaches the east boundary of the domain. On 8 and 9 April, the SO_2 emission largely decreases and SO_2 mass burden is moderate over La Réunion (1 to 3 DU). During this latter period, the simulation shows that the strong SO_2 mass burden modeled on 6 and 7 April, have been transported in the direction of the south of Madagascar and on the north east of the domain. An intense tongue, with a maximum of 20 DU, is extends over 2500 Km (bottom left of Fig. 4).

5.2 7 April, vertical SO_2 concentration

For detail the altitude of the main branches of the SO_2 plumes, the Fig. 5 display the SO_2 concentration and the horizontal wind field at different levels the 7 April 2007 at 12:00 UTC. Close to the surface, the alizes flux (6 m s^{-1} above La Réunion) turns the SO_2 plume towards the west of La Réunion. The surface SO_2 concentration modeled is low. This is due to the choice made in the definition of the bottom altitude of the column of SO_2, which permits to limit the extension of the plume on the west as for the observation OMI (Table 1). Close to the coast of Madagascar, the plume is more intense (10–20 ppbv) corresponding to the westerly plume of the 5 April. The winds field over La Réunion, rotate to be north-west in the layer comprises between 2000 m a.s.l. and 3000 m a.s.l., north at 4000 m a.s.l. and north east at 6000 m a.s.l. (Fig. 4). As a consequence the orientation of the SO_2 plume is strongly sheared and maxima location are dependent to the altitude level. At 4000 m a.s.l., the SO_2 maximum concentration located north of La Réunion (80 ppbv). At 6000 m a.s.l., the maximum concentration in the plume is greater to 400 ppbv.

At the upper part of the plume (6000 and 8000 m a.s.l.) the plume is advected at a large distance of La Réunion by north-east winds (10 to 15 m s^{-1}). At 8000 m a.s.l. the SO_2 maximum concentration decreases at 60 ppbv.

ACPD
10, 21357–21389, 2010

5.3 Acid formation and deposition

This part is dedicated to overview the distribution of dry deposition for SO_2 and H_2SO_4. Figure 6 gives the temporal integration of the SO_2 and H_2SO_4 mass deposed on the surface between 4 and 10 April. As observed in this figure the dry deposition occurred on the western part of the domain. Indeed, only this area is concerned by significant surface concentration of SO_2 that is advected by the alizes winds. Figure 6a indicates that the simulation model about 50 mg m^{-2} of SO_2 deposed in the vicinity of La Réunion, and 10 mg m^{-2} in a large tongue south east of Madagascar. The order of magnitude of SO_2 mass deposition in land of Madagascar is about 1 mg m^{-2}.

For H_2SO_4 (Fig. 6b), the location of the mass deposition is quite different from the SO_2. Indeed the H_2SO_4 (secondary species), is formed at distance in the plume of SO_2. As a consequences, the surface concentration of H_2SO_4 is located over the western part of the domain (not shown), and a maximum of 20 mg m^{-2} of sulfuric acid deposit, is simulated over the south east of Madagascar.

The total dry deposition over the simulation domain for SO_2 and H_2SO_4 is estimated to 22 Kt and 17.9 Kt respectively.

6 Mass budget and estimated flux

6.1 Mass budget

This last section is devoted to estimate the mass budget of the sulfur release in the atmosphere. Figure 7 gives the evolution of the integrated mass over the simulation domain for OMI (triangles and squares), and for the simulation (plain lines). OMI has observed an evolution of SO_2 mass very pronounced, from 10 Kt on 5 April, to 104 Kt (TRL) and 150 (TRM) on 7 April. After 7 April, the decreases of the SO_2 mass is strong and reached 40 Kt (TRL) and 90 Kt (TRM) on 8 April. Then the decreases of the SO_2 mass continuing, but less rapidly to reach 18 Kt (TRL) and 40 Kt (TRM) on 10 April.

ACPD
10, 21357–21389, 2010

The evolution of a tracer represented in Fig. 7 by the black solid line gives the evolution of an inert gas where no chemical transformation and deposition can occur. The maximum of this curve (144 Kt) is close to the upper SO_2 value recorded by OMI on 7 April using the TRM conditions. The mass simulated decreases after the mid day of 7 April, correspond to the mass escape through the domain boundary. It can be estimated to 40 Kt, but cannot explain the 110 Kt (TRM) of decreases observed by OMI during the period.

The evolution of SO_2 (blue solid line) differs to the tracer by two integrative processes; the chemical oxidation into H_2SO_4 and the dry deposition to the surface. Thus, the evolution of the SO_2 reaches a maximum at 135 Kt on 7 April and then decreases to 85 Kt. In parallel, the H_2SO_4 (red solid line) gradually increases to 28 Kt on April 10. The oscillation of the production of H_2SO_4 corresponds to the balance between oxidation of SO_2 that is efficient during day, and the loss by dry deposition or the escape through the domain boundaries. Nevertheless, the evolution of the SO_2 mass that integrates the loss at the surface, the oxidation and the escape out of the domain still overestimates at least by 45 Kt the mass observed by OMI at the end of the simulated period.

Another curve that filter every columns of SO_2 lower to 0.6 DU that corresponds to SO_2 OMI noise estimated by Krotkov et al. (2008), is added using the green solid line. The maximum modeled (125 Kt) fit perfectly with an average of TRL and the TRM observations. This is satisfying, because it means that the SO_2 mass is mainly located between 2.5 and 7.5 Km a.s.l., that corresponds to the layer where the main plumes are present. Indeed it is reasonable to assume that the order of magnitude of the SO_2 release in the atmosphere is well estimated by the model. Nevertheless, the decreases of the mass reach 65 Kt at the end of the simulation. It still 30 Kt more important than the observation by OMI with the TRM approach. Another filter fixed at 1 DU (orange solid line), gives similar results with a decrease slightly more important (60 Kt) but cannot reach the ending values of SO_2 observed by OMI. Note, that on 8 and 9 April, the mass modeled using this filter gives the same order of magnitude with

ACPD
10, 21357–21389, 2010

the observations using the TRM conditions. Nevertheless, the last differences between the observations and simulations cannot be explained by a detection limit greater than the theoretical value. Especially it is reasonable to assume that mass observed needs to be intermediate between the TRM and the TRL conditions.

In order to explain these differences, three hypothesis can be given that imply the presence of clouds during the period. First, clouds prevent the correct observation of the SO_2 and in a cloudy region the mass observed by OMI is systematically underestimated. This is convenient to Carn et al. (2008) results. This is clear for the 6 April where the weather over La Réunion and Maurice islands are cloudy (Fig. 2c), but this is also visible by the discontinuity on the observed plume the 7 April (Fig. 2d). Second, the presence of clouds imply the possible presence of precipitations that can scavenge the SO_2. By comparing the SO_2 simulated and observed in the Madagascar region on 8 and 9 April, (Figs. 4 and 2), we can assume that a non negligible part of SO_2 have been washed out. Third, the model do not integrate the aqueous chemistry that transform the SO_2 into H_2SO_4 in the cloud droplets. So, in cloudy areas, the formation of H_2SO_4 by the model is underestimated, and can explain a part of the overestimation of the SO_2 modeled during the last period.

6.2 Estimation of the SO_2 flux

The approach uses in the model to estimate the release of SO_2 in the atmosphere is based on a evolve concentration maintained in the model above Piton de la Fournaise (Sect. 4.3). From this approach, we can estimate the surface emission by considering that the emission must compensate the mass of SO_2 advected out of the column located above the eruption. It can be formulated upon using the initial flux F(0) and the iterative flux $F(t)$ defined (in $\mu g\,m^{-2}\,s^{-1}$) as:

$$F(0) = \frac{M_{SO_2}}{M_{air}\Delta t} \sum_{k=bot}^{top} \rho_k [SO_2]_k \Delta Z_k$$

ACPD
10, 21357–21389, 2010

and

$$F(t) = \frac{M_{SO_2}}{M_{air}\Delta X \Delta Y} \sum_{k=bot}^{top} \rho_k [SO_2]_k \Delta Z_k (u_k \Delta Y + v_k \Delta X - u_k v_k \Delta t)$$

where $[SO_2]_k$ is the SO_2 concentration at level k (in ppbv); Δt the time step of the model (s); M_{SO_2} and M_{air} represent the molecular weight for SO_2 and air respectively ($kg\,mol^{-1}$); ρ_k is the air density ($kg\,m^{-3}$); u_k and v_k is the zonal and meridian wind ($m\,s^{-1}$); and ΔX, ΔY, ΔZ_k is the grid size of the domain upon the axis west-east, south-north and upon the altitude (m). The index k represent the altitude level of the model.

Using this formulation, the SO_2 emission estimated by the model is given on Fig. 8. As shown, the model retrieve a strong evolution of the emission during 6 April reaching $2000\,kg\,s^{-1}$ over a surface of 20 by 20 Km^2 which corresponds to the surface of the horizontal grid of the model. This strong increases has to be linked to the increases of SO_2 concentration introduced in the eruptive column (Table 1). Note that this evolution of the emission is not smoothed due to the variability of the horizontal wind that entered in the formulation of the emission estimation. A day by day mass emission budget is also reported in Fig. 8. The mass emission during the main day of the eruption is 30.4 Kt, 89.2 Kt and 19.4 Kt for 5, 6 and 7 April respectively. The total emission during the period is 156.7 Kt of SO_2, and 147 Kt until 8 April. This latter value is comparable to the maximum mass of the tracer (144 Kt) simulated.

7 Conclusions

The originality of this study has two aims. First, it is devoted to analysis at the synoptic scale, the becoming of the SO_2 release in the atmosphere by the eruption of the Piton de la Fournaise. OMI observations show a strong variability in the mass of SO_2 over the domain. The first question is to understand what is the physical process able to

ACPD
10, 21357–21389, 2010

generate this strong variability. The simulation of the event using the mesoscale model MesoNH has given some answers. Several numerical 3-D tests of calibration of the model have been made using the observations of OMI and CALIPSO, and through the comparison of the large scale plumes given by MesoNH and OMI. The final result gives a correct representation of the main plumes by the model during the period 4–9 April 2007. As a consequences, the model has estimated the mass emitted in the atmosphere to 156 Kt of SO_2 during the period. Moreover, it has given some elements of answer to the becoming of the volcanic sulfur. During this event, the simulation has estimated to 45.9 Kt the oxidation of SO_2 into H_2SO_4, for which 17.9 Kt have been deposed at the surface by dry deposition. To this amount, it needs to add a sink of 22 Kt of SO_2 that have also deposed by dry deposition. By difference with the total amount of SO_2 present in the atmosphere at the end of the simulation (65 Kt), some 23 Kt of SO_2 have been escaped through the domain boundaries.

Nevertheless, these mass budget have to be taken with caution. Due to the resolution of the model that cannot represent correctly the cloud micro-physics, the aqueous process of scavenging by rain and the SO_2 transformation into acid in the cloud droplets are not taken into account in this study. As a consequences, the total deposition at the surface and the amount of acid formed is underestimated. Thus, the estimation of the SO_2release in the atmosphere on 6 April, where precipitations are present, is also probably underestimated. For these reasons, the values of SO_2 mass and the chemical transformation given by the model, have to be taken as a low limit of the reality.

The second aim of this study is to retrieve by a top-down approach, the SO_2 emission during the eruption. The approach consists to maintain an SO_2 concentration in a column located above the Piton de la Fournaise. Estimation of the SO_2 surface flux is then based on the fact that the emission flux is equal to the exportation of SO_2 out of the eruptive column. Using this method a strong variability of the SO_2 emission is retrieved, in particular with a peak on 6 April reaching 2000 $Kg\,s^{-1}$ on the surface model grid.

ACPD
10, 21357–21389, 2010

One important perspective of this study is to introduce this estimation of the surface flux in a high resolution simulations. Through high resolution studies,it will be possible to reproduce the local convection, the precipitations and the aqueous chemical transformation of gas that formed acid rains. These topics that linked the air pollution and their consequences on human health and ecosystems will constitute the future plans of this work.

Acknowledgements. We greatly acknowledge F. Caillé and R. Delmas for providing the pictures of the 2007, eruption. We thank L. Michon and N. Krotkov for their relevant comments. We also would like to thank the MesoNH assistance team for their support and availability and J. Kemp for improvement of the English.

The publication of this article is financed by CNRS-INSU.

References

Afe, O., Richter, A., Sierk, B., Wittrock, F., and Burrows, J.: BrO Emission from Volcanoes - a Survey using GOME and SCIAMACHY Measurements, Geophys. Res. Lett., 31, l24113, doi:10.1029/2004GL020994, 2004. 21359

Arellano, S., Hall, M., Samaniego, P., LePennec, J., Ruiz, A., Molina, I., and Yepes, H.: Degassing patterns of Tungurahua volcano (Ecuador) during the 1999–2006 eruptive period, inferred from remote spectroscopic measurements of SO2 emissions, J. Volcanol. Geotherm. Res., 176, 151–162, doi:10.1016/j.jvolgeores.2008.07.007, 2008. 21358

Baray, J., Ancellet, G., Taupin, F., Bessafi, M., Baldy, S., and Keckhut, P.: Subtropical

ACPD

10, 21357–21389, 2010

tropopause break as a possible stratospheric source of ozone in the tropical troposphere, J. Atmos. Solar-Terr. Phys., 60, 27–36, 1998. 21367
Barthe, C., Molini, G., and Pinty, J.: Description and first results of an explicit electrical scheme in a 3D Cloud Resolving Model, Atmos. Res., 76(1–4), 95–113, 2005. 21366
Bechtold, P., Bazile, E., Guichard, F., Mascart, P., and Richard, E.: A mass-flux convection scheme for regional and global models, Q. J. Roy. Meteor. Soc., 127, 869–886, 2001. 21366
Bougeault, P. and Lacarrere, P.: Parametrization of orography-induced turbulence in a meso-beta model, Mon. Weather Rev., 117, 1872–1890, 1989. 21366
Carn, S. A., Krotkov, N. A., Yang, K., Hoff, R. M., Prata, A. J., Krueger, A. J., Loughlin, S. C., and Levelt, P. F.: Extended observations of volcanic SO_2 and sulfate aerosol in the stratosphere, Atmos. Chem. Phys. Discuss., 7, 2857–2871, doi:10.5194/acpd-7-2857-2007, 2007. 21359, 21365
Carn, S., Krueger, A., Arellano, S., Krotkov, N., and Yang, K.: Ecuadorian volcanic degassing from space, J. Volcanol. Geotherm. Res., 176, 141–150, doi:10.1016/j.jvolgeores.2008.01.029, 2008. 21359
Clain, G., Baray, J. L., Delmas, R., Diab, R., Leclair de Bellevue, J., Keckhut, P., Posny, F., Metzger, J. M., and Cammas, J. P.: Tropospheric ozone climatology at two Southern Hemisphere tropical/subtropical sites, (Reunion Island and Irene, South Africa) from ozonesondes, LIDAR, and in situ aircraft measurements, Atmos. Chem. Phys., 9, 1723–1734, doi:10.5194/acp-9-1723-2009, 2009. 21367
Cohard, J. and Pinty, J.: A comprehensive two-moment warm microphysical bulk scheme II: 2D experiments with a non hysrostatic model, Q. J. Roy. Meteor. Soc., 126, 1843–1859, 2000. 21366
Coppola, D., Piscopo, D., Staudacher, T., and Cigolini, C.: Lava discharge rate and effusive pattern at Piton de la Fournaise from MODIS data, J. Volcanol. Geotherm. Res., 184, 174–192, doi:10.1016/j.jvolgeores.2008.11.031, 2009. 21361
Crassier, V., Suhre, K., Tulet, P., and Rosset, R.: Development of a reduced chemical scheme for use in mesoscale meteorological models, Atmos. Environ., 34, 2633–2644, 2000. 21366
Delmelle, P., Stix, J., Baxter, P., Garcia-Alvarez, J., and Barquero, J.: Atmospheric dispersion, environmental effects and potential health hazard associated with the low-altitude gas plume of Masaya volcano, Nicaragua, Earth Environ. Sci., 423–434, doi:10.1007/s00445-002-0221-6, 2002. 21358
Deroussi, S., Diament, M., Feret, J., Nebut, T., and Staudacher, T.: Localization of cavi-

ACPD
10, 21357–21389, 2010

ties in a thick lava flow by microgravimetry, J. Volcanol. Geotherm. Res., 184, 193–198, doi:10.1016/j.jvolgeores.2008.10.002, 2009. 21359, 21360

Diab, R., Thompson, A., Mari, K., Ramsay, L., and Coetzee, G.: Tropospheric ozone climatology over Irene, South Africa, From 1990 to 1994 and 1998 to 2002, J. Geophys. Res., 109, D20301, doi:10.1029/2004JD004793, 2004. 21364

Edmonds, M., Oppenheimer, C., Pyle, D., and Herd, R.: Rainwater and ash leachate analysis as proxies for plume chemistry at Soufrière Hills Volcano, Monserrat, in: Volcanic Degassing, edited by C. Oppenheimer, D. P. and Barclay, J., 213, 203–218, Geophysical Society, London Special Publication, 2003. 21359

Georgoulias, A., Balis, D., Koukouli, M., Meleti, C., Bais, A., and Zerefos, C.: A study of the total atmospheric sulfur dioxide load using ground-based measurements and the satellite derived Sulfur Dioxide Index, Atmos. Environ., 43(9), 1693–1701, doi:10.1016/j.atmosenv.2008.12.012, 2009. 21363

Grini, A., Tulet, P., and Gomes, L.: Dusty weather forecast using the MesoNH atmospheric model, J. Geophys. Res., 111, D19205, doi:10.1029/2005JD007007, 2006. 21366

Hoffman, D.: Perturbations to the global atmospehre associated with the El Chichón volcanic eruption of 1982, Rev. Geophys., 25, 743–759, 1987. 21358

Hoffman, D. J., Rosen, J., and Gringel, W.: Delayed production of sulfuric acid condensation nuclei in the polar stratosphere from El Chichon volcanic vapors, J. Geophys. Res., 90, 2341–2354, 1985. 21359

Khokhar, M., Frankenberg, C., VanRoozendael, M., Beirle, S., Kuhl, S., Richter, A., Platt, U., and Wagner, T.: Satellite observations of atmospheric SO2 from volcanic eruptions during the time-period of 1996–2002, Adv. Space Res., 36(5), 879–887, 2005. 21359, 21360

Krotkov, N., Carn, S., Krueger, A., Bhartia, P., and Yang, K.: Band residual difference algorithm for retrieval of SO_2 from the Aura Ozone Monitoring Instrument (OMI), IEEE T. Geosci. Remote Sens., 44(5), 1259–1266, 2006. 21362

Krotkov, N., McClure, B., Dickerson, R., Carn, S., Li, C., Bhartia, P., Yang, K., Krueger, A., Li, Z., Levelt, P., Chen, H., Wang, P., and Lu, D.: Validation of SO2 retrievals from the Ozone Monitoring Instrument over NE China, J. Geophys. Res., 113, D16S40, doi:10.1029/2007JD008818, 2008. 21362, 21371

Krueger, A., Walter, L., Bhartia, P., Schnetzler, C., Krotkov, N., Sprod, I., and Bluth, G.: Volcanic sulfur dioxide measurements from the total ozone mapping spectrometer instruments, J. Geophys. Res., 100(D7), 14057–14076, 1995. 21359

ACPD
10, 21357–21389, 2010

Kulmala, M., Laaksonen, A., and Pirjola, L.: Parametrization for sulfuric acid / water nucleation rates, J. Geophys. Res., 103(D7), 8301–8307, 1998. 21359

Lafore, J. P., Stein, J., Asencio, N., Bougeault, P., Ducrocq, V., Duron, J., Fischer, C., Héreil, P., Mascart, P., Masson, V., Pinty, J. P., Redelsperger, J. L., Richard, E., and Vilà-Guerau de Arellano, J.: The Meso-NH Atmospheric Simulation System. Part I: adiabatic formulation and control simulations, Ann. Geophys., 16, 90–109, doi:10.1007/s00585-997-0090-6, 1998. 21366

Lenat, J. and Bachelery, P.: Dynamics of Magma Transfer at Piton de La Fournaise Volcano (Réunion Island, Indian Ocean), in: Earth Evolution Sciences – Special Issue Modeling of Volcanic Processes, edited by: Chi-Yu and Scarpa, R., 57–72, Friedr. Vieweg and Sohn, Brauschweig/Wiesbaden, 1987. 21359

Lesouef, D., Gheusi, F., and Delmas, R.: Etude numérique des circulations locales á la Réunion: application aux transports de polluants, La Météorologie, 62, 32–38, 2008. 21368

Martin, R., Mather, T., Pyle, D., Power, M., Allen, A., Aiuppa, A., Horwell, C., and Ward, E.: Composition-resolved size distributions of volcanic aerosols in the Mt. Etna plumes, J. Geophys. Res., 113, D17211, doi:10.1029/2007JD009648, 2008. 21359

Masson, V.: A physically-based scheme for the urban energy balance in atmospheric models, Bound.-Lay. Meteorol., 94, 357–397, 2000. 21366

Mather, T., Pyle, D., and Oppenheimer, C.: Tropospheric Volcanic Aerosol, Geophys. Mono., 139, 189–212, doi:10.1029/139GM12, 2005. 21358

McCormick, M. P., Thomason, L. W., and Trepte, C.: Atmospheric effects of the Mt-Pinatubo eruption, Nature, 373, 399–404, 1995. 21358

Michon, L., Staudacher, T., Ferrazzini, V., Bachelery, P., and Marti, J.: April 2007 collapse of Piton de la Fournaise: a new example of caldera formation, Geophys. Res. Lett., 31, l21301, doi:10.1029/2007GL031248, 2007. 21360, 21361, 21367

Michon, L., Villeneuve, N., Catry, T., and Merle, O.: How summit calderas collapse on basaltic volcanoes: New insights from the April 2007 caldera collapse of Piton de la Fournaise volcano, J. Volcanol. Geotherm. Res., 184, 138–151, doi:10.1016/j.jvolgeores.2008.11.003, 2009. 21361

Noilhan, J. and Mahfouf, J.: The ISBA land surface parameterization scheme, Global Planet. Change, 13, 145–159, 1996. 21366

Oppenheimer, C., Pyle, D., and Barcley, J. (eds.): Volcanic degassing, vol. 213, Geophysical Society, London Special Publication, 2003. 21358

ACPD

10, 21357–21389, 2010

Peltier, A., Staudacher, T., Bachelery, P., and Cayol, V.: Formation of the April 2007 caldera collapse at Piton de La Fournaise volcano: Insights from GPS data, Volcanol. Geotherm. Res., 184, 152–163, doi:10.1016/j.jvolgeores.2008.09.009, 2009. 21359, 21361

Penner, J., Andreae, M., Annegarn, H., Barrie, L., Feichter, J., Hegg, D., Jayaraman, A., Leaitch, R., Murphy, D., Nganga, J., and Pitari, G.: Aerosols, their direct and indirect effects, Climate Change: The scientific basis, edited by: Houghton, J. T., Ding, Y., Griggs, D. J., Noguer, M., Van der Linden, P. J., Dai, X., Maskell, K., and Johnson, C. A., Cambridge University Press, UK, 289–349, 2001. 21359

Peuch, V., Amodei, M., Barthet, T., Cathala, M., Josse, B., Michou, M., and Simon, P.: MOCAGE : Modèle de Chimie Atmosphérique Grande Echelle, AMA, CNRM, Toulouse, France, 1999. 21367

Pollack, J., Toon, O., Danielsen, E., Hofmann, D., and Rosen, J.: The El Chichón volcanic cloud – an introduction, Geophys. Res. Lett., 10, 989–992, 1983. 21358

Robock, A.: Pinatubo eruption – The climatic aftermath, Science, 295, 1242–1244, 2002. 21358

SaintAnge, S.: La sédimentation volcanoclastique en contexte de point chaud (ile de La Réunion, Océan Indien), Thesis, University of La Reunion, France, 2009. 21360

Seifert, P., Gross, S., Ansmann, A., Freudenthaler, V., Hiebsch, A., Schmidt, J., Schnell, F., Tesche, M., and Wiegner, M.: Heterogeneous ice nucleation in the ash plume of Eyjafjoll observed at two central-European EARLINET lidar sites., in: The 13th Conference on Cloud Physics/13th Conference on atmospheric Radiation (28 June–2 July 2010), AMS, Portland, USA, 2010. 21358

Seinfeld, J. and Pandis, S.: Atmospheric Chemistry and Physics, Second edition, Wiley interscience pub, 2006. 21359, 21365

Staudacher, T., Ferrazzini, V., Peltier, A., Kowalski, P., Boissier, P., Catherine, P., Lauret, F., and Massin, F.: The April 2007 eruption and the Dolomieu crater collapse, two major events at Piton de la Fournaise (La Runion Island, Indian Ocean), J. Volcanol. Geotherm. Res., 184, 126–137, doi:10.1016/j.jvolgeores.2008.11.005, 2009. 21360, 21361

Stevenson, D., Johnson, C., Collins, W., and Derwent, R.: The tropospheric sulphur cycle and the role of volcanic SO_2, Geological Society special publication, 213, 295–305, 2003. 21359, 21365

Suhre, K., Mari, C., Bates, T., Johnson, J., Rosset, R., Wang, Q., Bandy, A., Blake, D., Businger, S., Eisels, F., Huebert, B., Kok, G., Mauldin, R. I., Prévôt, A., Schillawski, R., Tanner, D., and

ACPD

10, 21357–21389, 2010

Thornton, D.: Physico-chemical modeling of the First Aerosol Characterization Experiment (ACE 1) Lagrangian B, 1. A moving column approach, J. Geophys. Res., 103, 16433–16455, 1998. 21366

Sutton, A., Elias, T., Gerlach, T., and Stokes, J.: Implications for eruptive processes by sulphur dioxide emissions from Kilauea Volcano, Hawaii, J. Volcanol. Geotherm. Res., 108, 283–302 and 423–434, 2001. 21359

Thomas, H., Watson, I., Carn, C. K. S., and Murray, S.: A multi-sensor comparison of sulphur dioxide emissions from the 2005 eruption of Sierra Negra volcano, Galapagos Islands, Remote Sens. Environ., 113, 1331–1342, doi:10.1016/j.rse.2009.02.019, 2009. 21359

Tulet, P., Crassier, V., Solmon, F., Guedalia, D., and Rosset, R.: Description of the MESOscale NonHydrostatic Chemistry model and application to a transboundary pollution episode between northern France and southern England, J. Geophys. Res., 108(D1), 4021, doi:10.1029/2000JD000301, 2003. 21366

Tulet, P., Crassier, V., Cousin, F., Shure, K., and Rosset, R.: ORILAM, A three moment lognormal aerosol scheme for mesoscale atmospheric model. On-line coupling into the MesoNH-C model and validation on the ESCOMPTE campaign, J. Geophys. Res., 110, D18201, doi:10.1029/2004JD005716, 2005. 21366

Winker, D. M., Pelon, J., and McCormick, M.: The CALIPSO mission: Spaceborne lidar for observation of aerosols and clouds, Symposium on Remote Sensing of the Atmosphere, Environment and Space, Hangzhou, China, 23–27 October 2002, 4893, 1–11, 2003. 21365

Yang, K., Liu, X., Krotkov, N., Krueger, A., and Carn, S.: Estimating the altitude of volcanic sulfur dioxide plumes from space borne hyper-spectral UV measurements, Geophys. Res. Lett., 36, l10803, doi:10.1029/2009GL038025, 2009. 21362, 21365

ACPD

10, 21357–21389, 2010

Table 1. Evolution of the column size and the SO_2 concentration introduced in the model over La Réunion between 4 and 10 April 2007.

Day of April, 2007	4	5	6	6	6	6	7	8	9	10
Hours (UTC)	11	11	2	7	14	18	6	11	10	11
Bottom (m a.s.l.)	surface	500	3000	3500	4000	4000	3500	500	surface	surface
Top (m a.s.l.)	2000	5000	8000	9000	9000	8000	8000	4000	2500	2500
SO_2 (ppbv)	46	205	554	1091	462	346	205	40	37	37

ACPD
10, 21357–21389, 2010

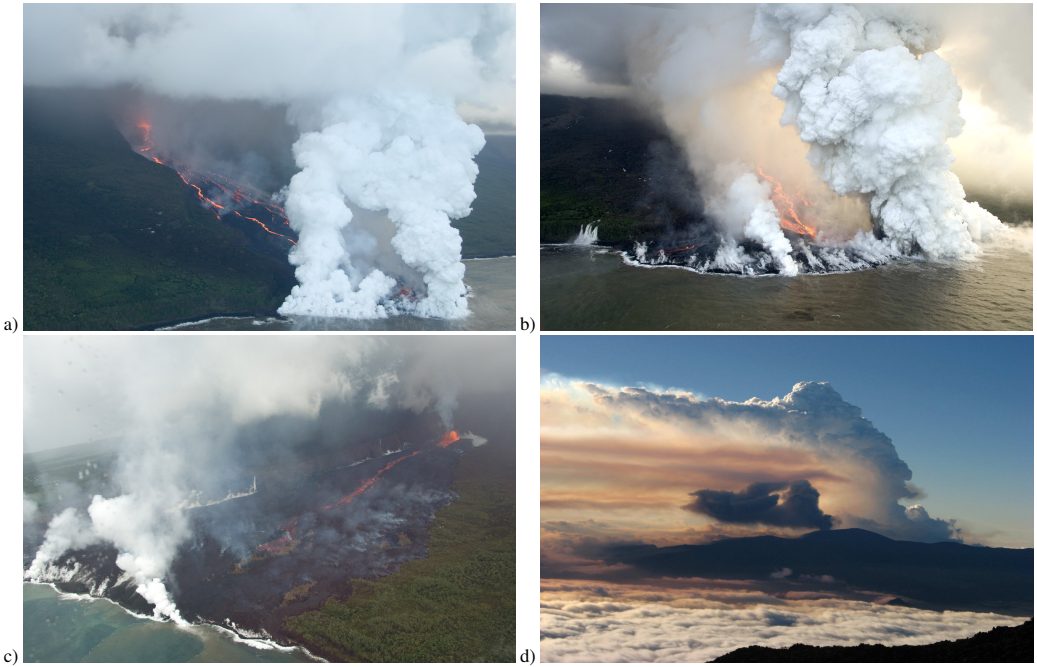

Fig. 1. (a, b and **c)** Lava flow on the Grand Brûlé area near the Piton Tremblé crater respectively on 5, 6 and 8 April 2007. Copyright F. Caillé. **(d)** Three different plumes over the Piton de la Fournaise during the collapse of the Dolomieu crater on 6 April 2007. Copyright R. Delmas.

ACPD
10, 21357–21389, 2010

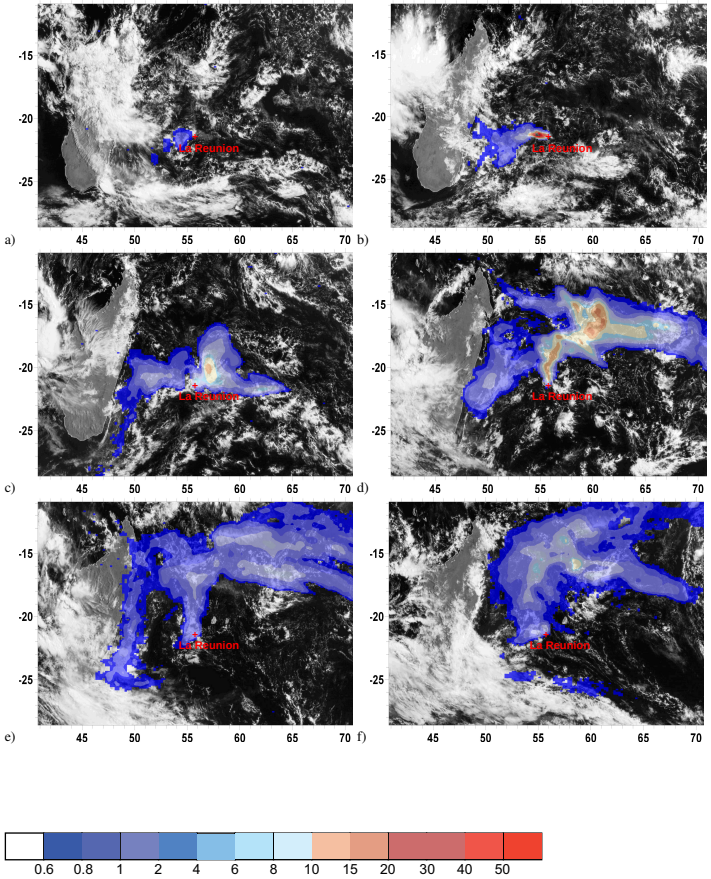

Fig. 2. SO_2 mass burden (Dobson Units) measured by OMI superimposed with the meteosat visible channel, on 4 April at 11:00 UTC **(a)**, 5 April at 10:00 UTC **(b)**, 6 April at 11:00 UTC **(c)**, 7 April at 10:00 UTC **(d)**, 8 April at 11:00 UTC **(e)** and 9 April at 10:00 UTC **(f)**.

ACPD
10, 21357–21389, 2010

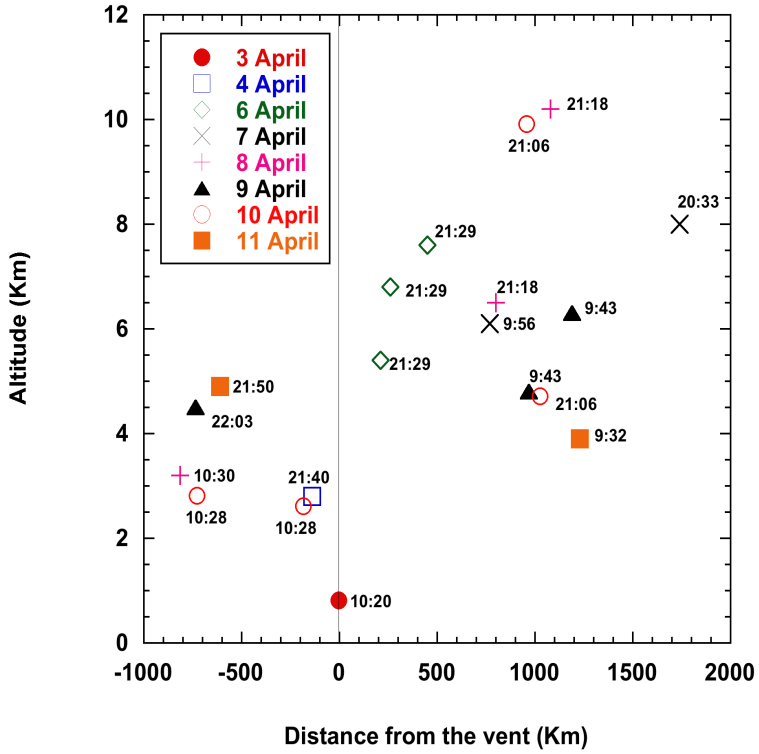

Fig. 3. Altitude and distance from La Réunion of the aerosols plumes observed by CALIOP sensor on CALIPSO satellite from 3 April to 11 April 2007 (negative abcisse values corresponds to the west, and positive values to the east).

ACPD
10, 21357–21389, 2010

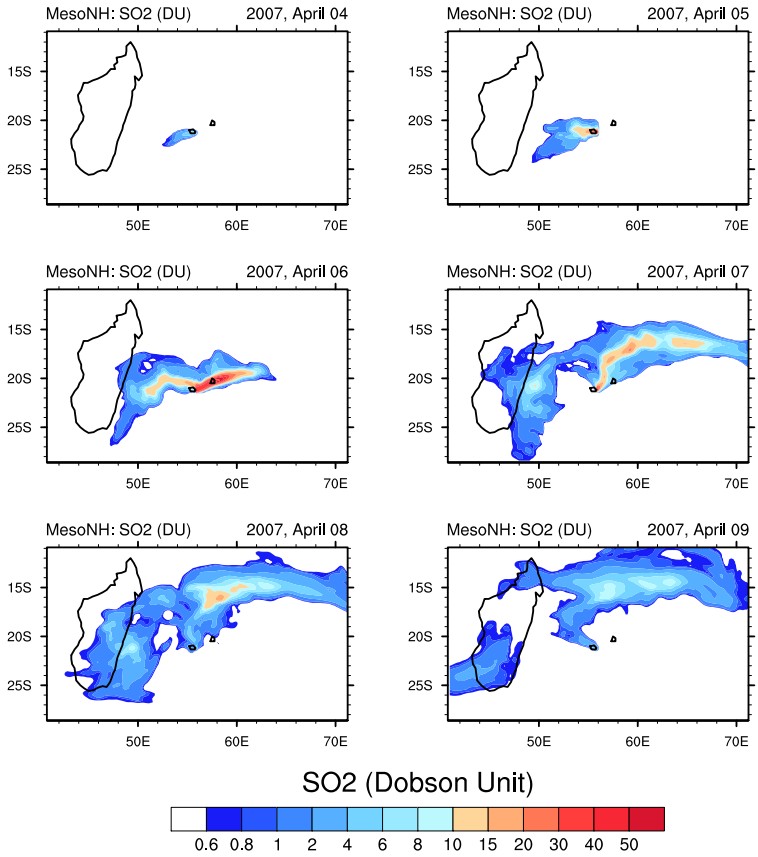

Fig. 4. Evolution of SO_2 mass burden simulated by MesoNH at 12 UTC between 4 and 9 April 2007.

ACPD
10, 21357–21389, 2010

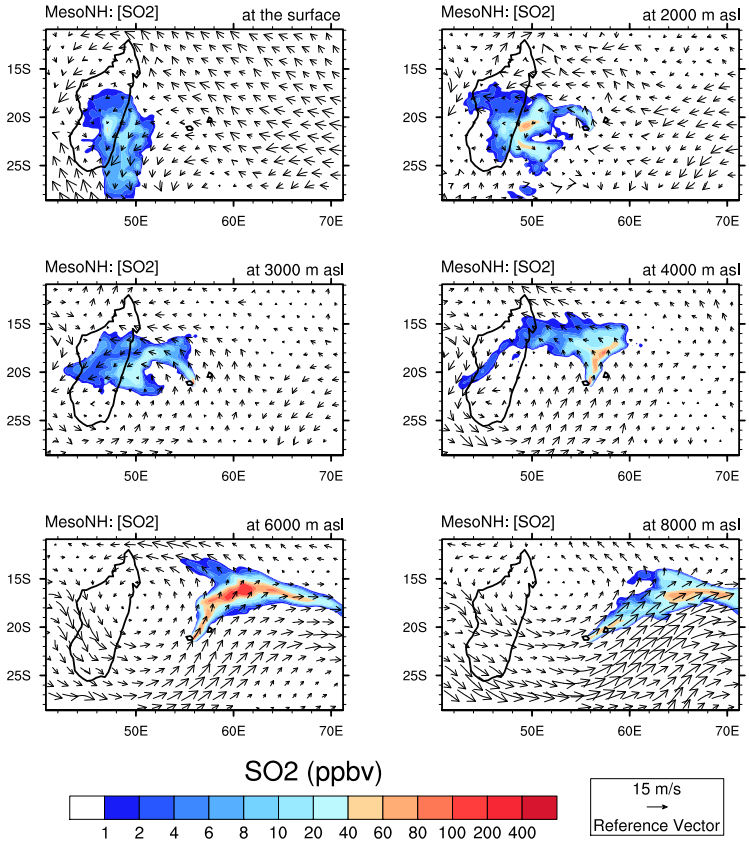

Fig. 5. Concentration of SO_2 (ppbv) and horizontal wind (vector) at different levels simulated by MesonH on 7 April 2007.

ACPD
10, 21357–21389, 2010

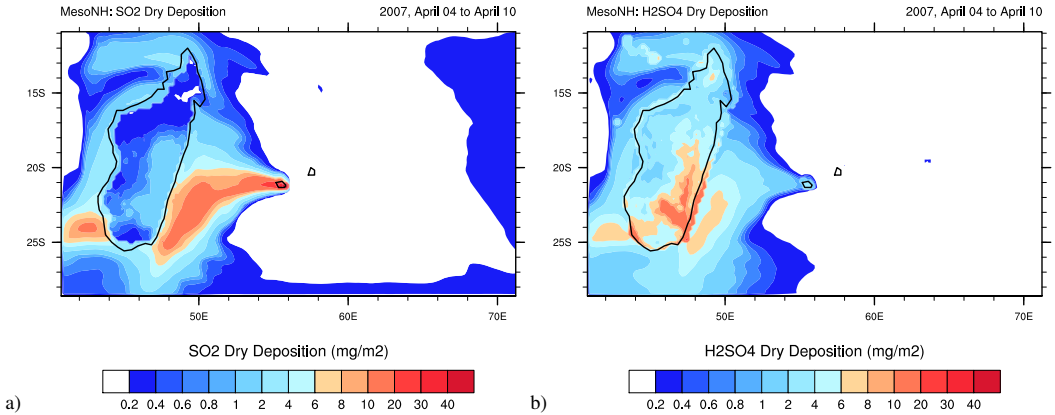

Fig. 6. Surface dry deposition of SO_2 **(a)** and H_2SO_4 **(b)** ($mg\,m^{-2}$), of SO_2 (a) and H_2SO_4 (b), simulated by MesoNH between 4 and 11 April 2007.

ACPD
10, 21357–21389, 2010

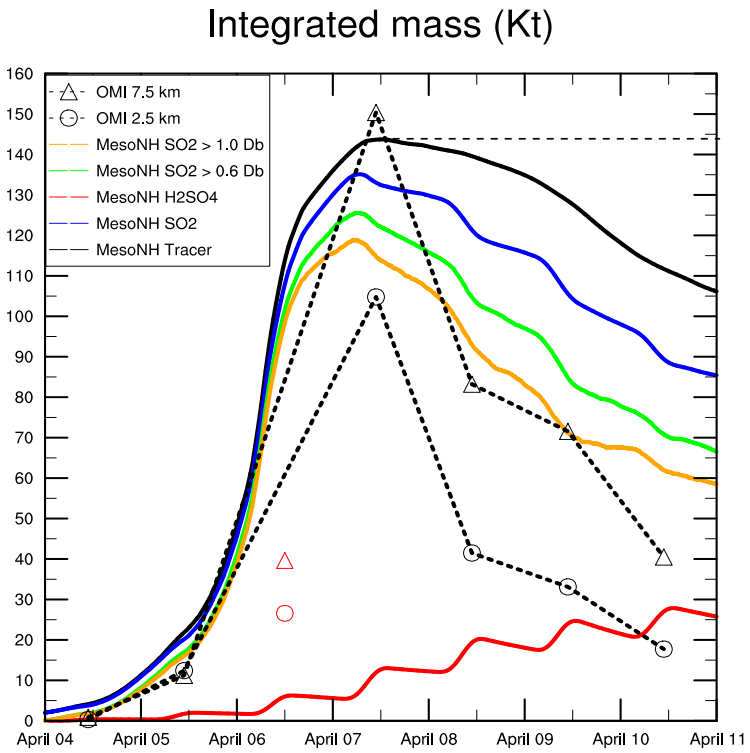

Fig. 7. Sum of the mass (Kt) simulated by MesoNH on the whole domain (solid lines) and observed by OMI (dashed lines with triangles and circles) between 4 and 11 April 2007.

ACPD
10, 21357–21389, 2010

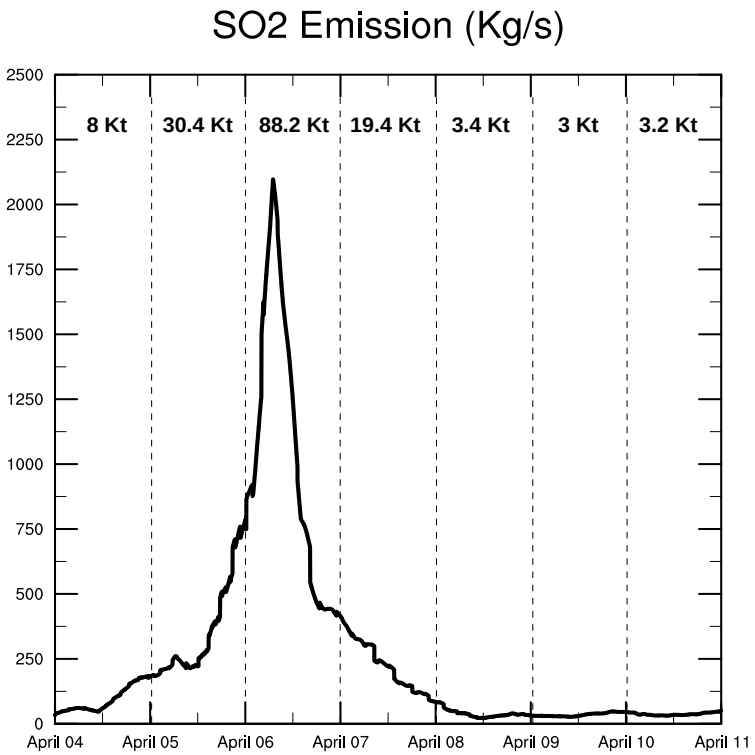

Fig. 8. Evolution of the SO_2 emission ($Kg\,s^{-1}$) estimated by MesoNH between 4 and 11 April 2007. Upper values correspond to daily mass of SO_2 (Kt) emitted during the period.

ACPD
10, 21357–21389, 2010